The Mutual Interactions of Carbon Nanotubes During Dielectrophoresis

Ali Kashefian Naieni, *Student Member, IEEE*, and Alireza Nojeh, *Member, IEEE*

Abstract—Dielectrophoresis (DEP) has been widely used for the deposition of various types of nanomaterials including carbon nanotubes (CNTs). Here, we report the results of experiments that show that the interactions between deposited and suspended nanotubes during the deposition process can considerably affect the dynamics and the final results of the deposition. Semiperiodic stripes of nanotubes bridging two electrodes are formed from solutions containing no surfactant. The periodicity of the patterns depends on the geometry of the electrodes. Finite-element method simulations are used to explain the mechanisms underlying the observed experimental outcomes. The pattern formation is shown to be related to the mutual effects of CNTs on each other. The reason lies in the changes in the electric field as a result of deposition of CNTs. These changes directly alter the DEP force field and, therefore, the way the CNTs are guided. The extent of effectiveness of the electrothermal force, which turns out to be substantial for some solutions, is also investigated, and it is shown that although in some situations the heat generated by the current passing through the nanotubes considerably increases this force, the DEP force remains dominant when a surfactant-free solution is used.

Index Terms—Carbon nanotube, deposition from solution, dielectrophoresis, finite-element method.

I. INTRODUCTION

CARBON nanotubes (CNTs) have been prominent stars in the research scene since their discovery. While their promising properties make them a potential candidate for a wide range of applications, the unresolved fabrication challenges hinder their applicability in commercial products in the near future, and more investigation into the existing obstacles on the way to reliable and repeatable fabrication is needed.

Dielectrophoresis (DEP) is one of the popular methods for fabricating micro- and nanoparticle-based devices from solutions [1]–[3]. CNT devices made with DEP range from single nanotubes to small mats [4]–[6]. The low-temperature nature, relatively good control over the position and density of the deposited nanotubes, simplicity of the required equipment, and availability of solutions containing particular types of CNTs

are some of the advantages of DEP over other CNT fabrication methods such as chemical vapor deposition.

Despite all the advantages, DEP-fabricated devices are far from being perfectly reproducible, and more research on the effectiveness of various parameters is needed, especially on topics such as the role of solution conductivity, and the effects that CNTs exert on each other during deposition, which have by and large been neglected so far.

We have previously reported that the solution properties and electrode shapes, among other parameters, significantly affect the DEP results [7]. While the DEP force plays the major role in the close proximity of the gap between the electrodes, other forces such as the electrothermal force agitate the liquid environment and particularly alter the long-range movement of the nanotubes and affect the deposition patterns for solutions with high conductivity. For aqueous solutions with no surfactant, the heat generated because of the current passing through the medium is considerably less than the previous case and, therefore, the electrothermal force is suppressed, leaving the DEP force as the dominant factor in the nanotubes' motion and deposition.

When low-conductivity solutions are used for making CNT devices on electrodes with a few tens of micrometers in width, the deposited nanotubes show a distinct periodic pattern (see [8, Fig. 4] or [9, Fig. 1]). This is especially more pronounced in cases where there is a considerable gap between the electrodes (see [10, Fig. 2]).

Vijayaraghavan *et al.* stated that the deposition of a CNT on sharp electrodes results in a change in the DEP force around the electrodes from attraction to repulsion during the rest of the process [11]. While this may be the case for sharp electrodes, it cannot explain why the stripes in wide electrodes are made of multiple nanotubes; an opposite mechanism appears to be at play in this case.

There are two scenarios that can potentially explain the formation of nanotube stripes: the alteration of the electric field around the deposited nanotubes, and/or the alteration in the movement of the solution around the electrodes and the deposited CNT due to the change in the temperature profile because of the high current passing through the deposited nanotubes.

Here, we reveal the mechanism of pattern formation due to the mutual interactions of nanotubes through a quasi-static study of the evolution of the device during the DEP deposition process from low-conductivity solutions. The results of this combined experimental-simulation study take us one step closer toward engineering the morphology of CNT-based devices.

We first report the results of experiments using devices with different gap lengths between the electrodes and different deposition times to investigate the described effect in more

detail. Three-dimensional (3-D) finite-element simulations are used to elucidate the mechanism behind the deposition of nanotubes in striped patterns.

The experiments show a clear trend in the formation of the stripes from the very beginning of the process. Throughout the DEP experiments, the stripes attract more nanotubes and expand their width. These stripes have a periodicity, which depends on the geometry of the sample. The results of different scenarios for nanotube deposition are presented here. In each case, the DEP force, as well as the electrothermal motion of the CNTs, is investigated. The results show that, while the electrothermal force is greatly enhanced when there is a CNT bridging the two electrodes, the interaction between the suspended nanotubes and the electric field altered by the deposited nanotubes—even if the latter do not bridge the electrodes—plays the key role in the formation of the patterns. Parts of the results of this study have been presented at a recent conference [12].

II. METHODOLOGY

A. Fabrication of the Electrodes

The electrodes were patterned using photolithography on a highly p-doped [100] silicon wafer with 2 μm of thermally grown oxide on top, followed by electron beam evaporation of 20 nm of chromium and 50 nm of palladium. The chromium layer enhanced the adhesion of the metal layer on the oxide, while the purpose of the palladium layer was to make devices with Ohmic contact between the electrodes and the nanotubes.

The electrodes were 50 μm wide near the gap region. Three different types of devices with 4, 8, and 20 μm of gap between the opposing electrodes were used for the DEP experiments. The electrodes in all devices were connected to larger pads made during the same process as the electrodes. These pads were used as contacts for micromanipulator probes to electrically connect the electrodes to the outside world for the DEP experiments, and potentially for electrical characterization of the devices.

B. Dielectrophoresis Experiments

The CNT solution was prepared by diluting a commercially available, surfactant-free aqueous CNT solution from NanoLab, Inc., [13]. The final CNT concentration in the solution was 2.5 μg/ml. The suspended nanotubes had a length in the range of 1–5 μm and an average diameter of 1.5 nm.

The DEP experiments were performed by applying a potential difference with a frequency of 500 kHz to the electrodes while the sample was immersed about 3 mm deep in the solution. The applied voltages were chosen so as to maintain an applied electric field of 1 V/μm between the electrodes. After the deposition, the samples were rinsed with deionized water and blow-dried with nitrogen.

C. Finite-Element Simulations

To capture the 3-D nature of the problem, and to be able to investigate the changes of the forces in different directions, 3-D finite-element simulations were performed using COMSOL Multiphysics software package [14]. Because of the limitation

on the total number of points that could be used for meshing due to the computationally expensive character of the 3-D simulations, the size of the structure needed to be small. A 16 μm $\times$ 20 μm $\times$ 10 μm structure (x, y, and z directions, respectively) represented the solution and was placed over a pair of 70-nm-thick electrodes, which were 4 or 8 μm apart in the y direction. The substrate was represented by a 2-μm-thick silicon dioxide slab. The potential of the backside of this layer was set to emulate the potential of the highly doped part of the silicon wafer.

The potential and the electric field in the system were computed by solving quasi-static Maxwell's equations with the electrodes' potentials set to $\pm$V/2 and the back gate being grounded. Electrical insulation was used as the boundary condition on all the outer boundaries of the system, i.e., the perpendicular component of the current was equal to zero at these boundaries. Since the magnitude of the gradients of the potential was sizable in the gap between the electrodes but not near the edges, this boundary condition seems reasonable. Once the electric field was calculated, the DEP force was derived using

$$\langle \overrightarrow{F}_{\mathrm{DEP}} \rangle = \frac{\pi abc}{3} \varepsilon_m \mathrm{Re} \left\{ \frac{\varepsilon_p^* - \varepsilon_m^*}{\varepsilon_m^*} \right\} \nabla |\overrightarrow{E}|^2 \qquad (1)$$

in which $\vec{F}_{\mathrm{DEP}}$ denotes the DEP force on the nanotubes, a, b, and c are half of the lengths of the major ellipsoid axes representing the CNT, E is the electric field, and ε_p^* and ε_m^* are the CNT and surrounding medium's complex permittivities, respectively [15].

The electric field results in a current passing through the solution, which in turn leads to heat generation because of the Joule heating phenomenon. Another source of heat can be the current passing through CNT/CNTs bridging the two electrodes. Even though the transport of charge carriers is considered to be ballistic for pristine nanotubes, they normally have defects (especially the solution-processed ones) which give them a finite resistance [16]. The generated heat creates a nonuniform temperature profile. Using the following energy balance equation, the temperature at each point was found:

$$k\nabla^2 T + Q = 0 \qquad (2)$$

where k is the thermal conductivity, Q is the generated heat power, and T denotes the temperature. Zero temperature gradient at the outer boundaries was used as the boundary condition. The electrodes were assumed to be thick enough to be able to keep a constant temperature equal to the ambient.

The temperature gradient results in gradients in the physical properties of the medium such as the conductivity and permittivity. In the presence of an electric field, these changes result in a body force on the solution, which is known as the electrothermal force. Depending on the magnitude of the gradient of the permittivity and conductivity, which in turn depend on the magnitude of the temperature gradient, and also the electric field at each point, the electrothermal force varies at different points; this force can create significant agitation in the solution. The time-averaged value of the electrothermal force per unit volume was calculated using the following expression in which the permittivity and conductivity gradients are written in terms

of the temperature gradient:

$$\langle \vec{F}_{ETF} \rangle = \frac{1}{2}\left[(\alpha - \beta)(\nabla T . \vec{E})\frac{\varepsilon \vec{E}}{1+(\omega\tau)^2} - \frac{1}{2}|\vec{E}|^2 \varepsilon \alpha \nabla T\right]$$
(3)

in which $\alpha = \partial\varepsilon/\varepsilon\partial T = -0.4\%$, and $\beta = \partial\sigma/\sigma\partial T = 2\%$ per Kelvin for an aqueous solution. $\tau = \varepsilon/\sigma$ is the charge relaxation time in the solution.

The velocity of the movement of an incompressible fluid with a low Reynolds number being affected by a volumetric force can be computed using a combination of the Navier–Stokes and mass conservation equations as follows:

$$\eta\nabla^2\vec{u} - \nabla p + \vec{F} = 0$$
(4)

and

$$\nabla.\vec{u} = 0$$
(5)

where η is the solution viscosity, p is the pressure, $\vec{u}$ is the velocity vector, and $\vec{F}$ is the general volumetric force, which is the electrothermal force here.

The movement of particles (CNTs in this study) is governed by

$$m\frac{d\vec{u}_{CNT}}{dt} = -f(\vec{u}_{CNT} - \vec{u}) + \vec{F}_{DEP}$$
(6)

in which f is the friction factor, m is the mass of the CNT, $\vec{u}$ is the solution velocity, and $\vec{u}_{CNT}$ is the total velocity of the nanotubes.

$$f = \frac{3\pi\eta l}{\ln(l/r)}$$
(7)

where l and r are the length and radius of a rod moving randomly in the solution.

The terminal velocity (beyond which the velocity of the CNTs would not change if the forces remain constant) is eventually reached and is equal to

$$\vec{u}_{CNT} = \vec{u} + \frac{\vec{F}_{DEP}}{f}.$$
(8)

III. RESULTS AND DISCUSSION

To reach a clear understanding of the dynamics of deposition of nanotubes, a series of DEP experiments with time durations ranging between 15 s and 4 mins were performed using electrodes with 8 μm of gap between them. Fig. 1 shows the scanning electron microscopy (SEM) viewgraphs of the deposited nanotubes between the two electrodes. The results show a clear trend in the formation of CNT stripes from the very beginning. The stripes start to take shape even for the shortest experiment with a time of $t = 15$ s. Since the gap between the two electrodes is almost twice as large as the length of the longest nanotubes suspended in the solution, the stripes can bridge only if two or more (often several) nanotubes connect in alignment with each other. For longer deposition times, the half bridging CNTs turn into fully bridging stripes, and from then on the stripes thicken until the whole gap is covered.

The overall process of CNT deposition on the electrodes seems to start by the deposition of nanotubes on the edge of the
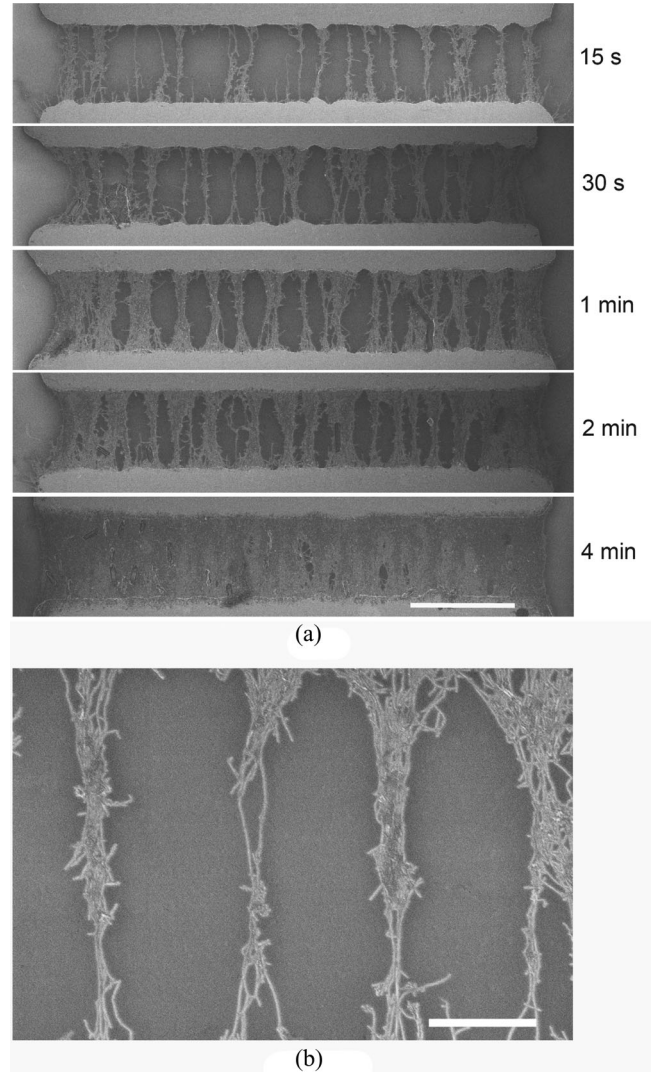

Fig. 1. (a) SEM images of the deposition patterns for different times. The gap between the electrodes is 8 μm. The scale bar is 10 μm. (b) Magnified view of the DEP result for t = 30 sec device. The scale bar is 2 μm.

electrodes. Other CNTs are then deposited in alignment with the previously deposited nanotubes to form bridges between the two electrodes. The stripes formed are parallel to each other. The number of stripes forming between the two electrodes and, therefore, the distance between them, seem to be almost equal for different experiments. Considering that the results shown in Fig. 1 are from different devices, each used for DEP separately, the consistent trend observed means that the number of stripes shaped between the electrodes during DEP is not random and the results of the process are repeatable. Once the stripes are formed, other nanotubes are attracted toward them (especially toward the nanotubes-electrode contact region), and deposit on the edges of the stripes until they fill the gap. The ratio of the area covered by the nanotubes to the surface between the two electrodes increases almost linearly with a rate of 25 percent per minute. Moreover, the results of atomic force microscopy performed on the devices show a clear 2-D expansion for the stripes: the nanotubes mostly deposit beside the stripes rather
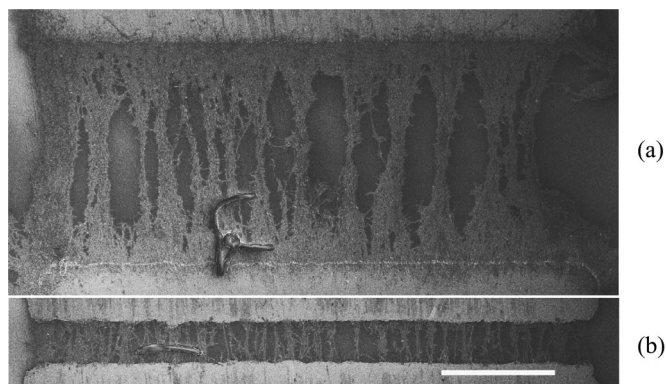
Fig. 2. SEM images of the deposition patterns using 4 min of deposition time and devices with (a) 20 μm and (b) 4 μm of gap. The scale bar is 10 μm.
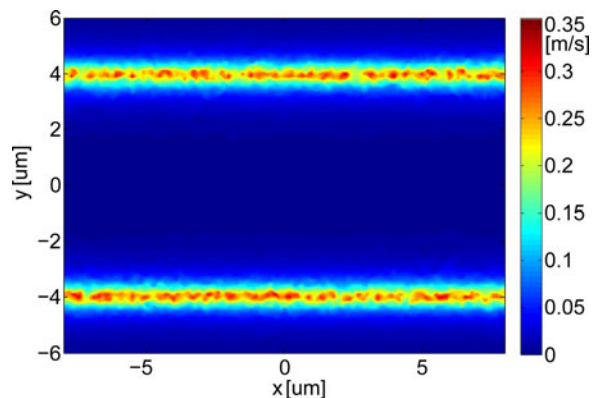

Fig. 3. Magnitude of the velocity of the nanotubes on a plane 400 nm above the substrate surface and parallel to it.

Fig. 4. Same as in Fig. 3, but in the presence of a deposited nanotube half-bridging the gap.

than creating stripes consisting of multiple layers. In all cases, the maximum heights of the stripes are in the range of 15–20 nm, with variations of a few nm from device to device.

Similar experiments were performed with devices with 4 and 20 μm gaps. Fig. 2 shows the results when $t = 4$ min. The experiments were performed on two devices for each time setting. The results show good reproducibility especially for devices with longer durations. For shorter times (15 and 30 s) the stripes are not fully formed yet and the number of bridges between the electrodes can be different for different devices with the same experimental settings. Although the overall look of the samples is the same and the CNTs create stripes during deposition, the gap between the stripes is different for devices with different gap distances. While the distance between adjacent stripes is in the range of 2.8 to 3.2 μm when the gap between the electrodes is 8 μm, it is in the range of 3.6 to 4 μm when the gap is 20 μm and less than 1.8 μm for 4 μm of gap. Also, the phenomenon is not as pronounced in 4-μm-gap devices as it is in devices with larger gaps. It seems that the periodicity of the stripes depends on the geometry of the sample.

To understand the various steps of the nanotube deposition process, finite-element simulations were carried out for devices with 4 and 8 μm of gap for three cases: no nanotube, one nanotube half bridging, and one nanotube fully bridging the gap. In the second and third case, a rectangular prism with a 2 nm $\times$ 2 nm cross section was used to emulate the CNT bridging/half bridging the gap between the electrodes. For the case of a CNT half bridging the gap, the potential of the CNT was set equal to the potential of the electrode that it was connected to. When the CNT was connected to both of the electrodes, the potential of the rectangular prism surface was set to ground. This value was chosen based on a work by Chen *et al.* in which it is shown that the potential drop on a metallic nanotube bridging two electrodes happens primarily within 5 nm of the nanotube–metal junction at each side [17] and, therefore, almost the entire nanotube body is at the average potential of the two electrodes, which is zero in our case.

Fig. 3 shows the velocity of the nanotubes in the solution on an xy plane (parallel to the substrate surface), 400 nm above the substrate when no CNT has deposited yet. The gradient of the electric field is highest around the edges of the electrodes
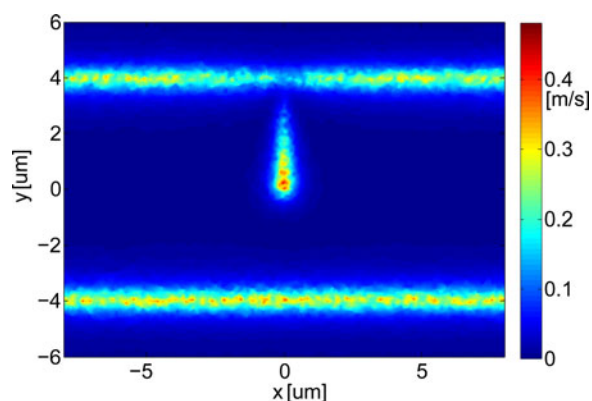
and therefore the CNTs are mainly attracted toward there at this stage.

The velocity of the CNTs in the half-bridging nanotube situation in the same plane as in the previous figure is shown in Fig. 4. The nanotubes' motion is clearly affected by the presence of the deposited nanotube and the DEP force pushes the suspended nanotubes toward the tip of the deposited nanotube. This is due to the very high aspect ratio of the CNT, which considerably enhances the electric field on the tip, and results in a larger DEP force around it. This argument can explain why the half bridging nanotubes attract other nanotubes to deposit aligned and connected with them toward the opposite electrode.

A detailed view of the velocity components for the case of a bridging nanotube is shown in Fig. 5. The x (parallel to the electrode edges) and z (vertical direction) components of the velocity of the nanotubes at two different heights from the surface of the substrate are presented. At 500 nm above the surface, the x component of the velocity pushes the suspended CNTs away from the deposited nanotube in the central regions of the gap. The z component is very low (compared to part d of the same image) at this height.

Fig. 5(c) and (d) shows the velocity components 50 nm away from the substrate surface. The x component attracts the suspended CNTs toward the deposited nanotube especially near the edges; only in a very small region around the center of the
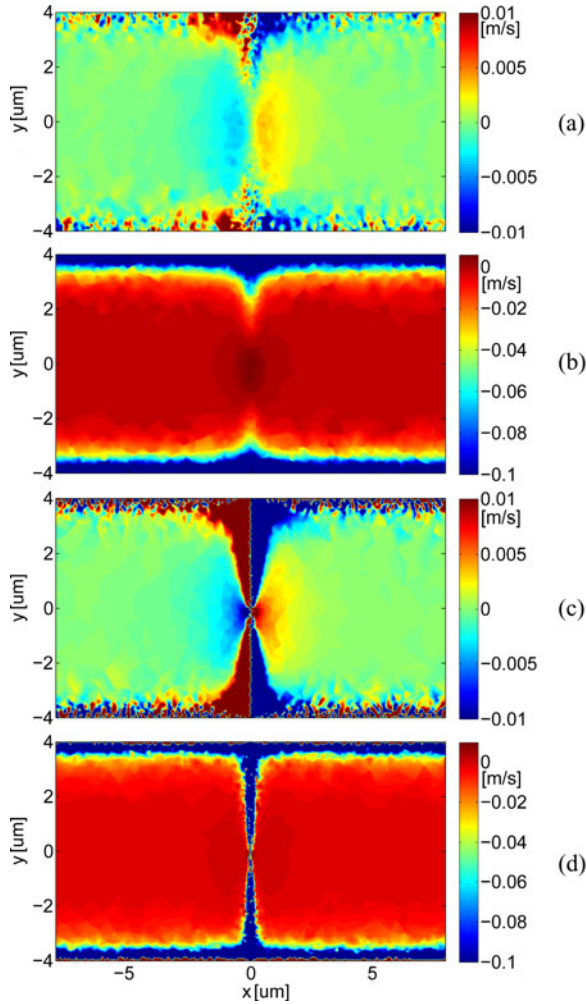
Fig. 5. Components of the velocity of the nanotubes in planes parallel to the substrate surface: (a) x and (b) z components in the plane at a height of 500 nm above the surface, (c) x and (d) z components in a plane 50 nm high.
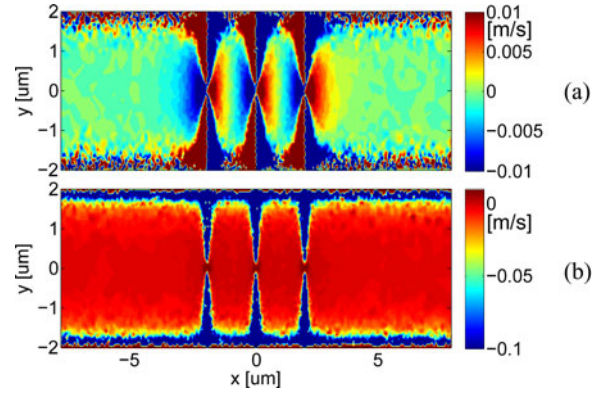

Fig. 6. Components of the velocity of the nanotubes in a plane parallel to the substrate surface and 50 nm above it in the case with three CNTs already deposited: (a) x and (b) z components.
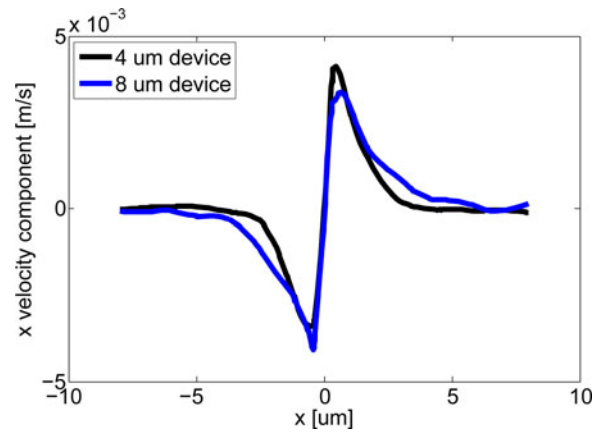

Fig. 7. x component of the velocity for 4 - and 8-μm-gap devices on a line parallel to the edges of the electrodes in the middle of the gap at a height of 500 nm above the substrate surface.

gap is this force repulsive. The z component is strongly negative (toward the surface) in the close vicinity of the deposited CNT and pins the suspended CNTs in that region to the surface. As a result, the suspended nanotubes are attracted toward (especially the base of) the fully bridging deposited nanotubes and, once they are close to the edge of the latter, a very large DEP force makes them deposit. Thus, the combined effects of these two components explain the peculiar shape of the nanotube stripes and their thickening near the electrodes (see the experimental results of Figs. 1 and 2 for the shape of the stripes).

Similar simulations were performed for devices with 4 μm of gap between the two electrodes. A particular case with three nanotubes deposited at a distance of 2 μm from each other was simulated for the 4-μm-gap device as well. Simulating an equivalent structure with a larger gap was not possible due to the computational limitations. The velocity components of the CNTs on a plane 50 nm above the substrate and parallel to it are shown in Fig. 6. Again the nanotubes are attracted toward the base of the deposited CNTs. It should be noted that the x-component of the force around the middle of the gap is more repulsive compared to the area around the nanotube–electrode connection. The shorter nanotubes feel the force as shown in the

figure, but the longer nanotubes align themselves with the field prior to deposition and experience an average force, which is determined by the electric field and solution motion along their entire lengths. The diamond-shaped empty regions seen in Fig. 6 bear a striking resemblance to the empty regions in-between the nanotube stripes seen in the experimental results shown in Figs. 1 and 2, a confirmation that the simulations are, indeed, capturing the mechanism behind the pattern formation process.

Fig. 7 shows the x velocity component of the nanotubes due to the DEP force on a line parallel to the edges of the electrodes in the middle of the device at a height of 500 nm from the surface for both the 4 and 8-μm-gap devices. It can be seen that the extent for which the CNTs are pushed away for the latter device is almost double that for the former. This can explain the difference in the distance between the stripes in these two devices.

As mentioned earlier, we have previously demonstrated that the solution motion caused by inhomogeneities induced by the nonuniform temperature profile—especially the movement of the solution because of electrothermal force—can be a substantial factor in the deposition pattern of nanotube devices made using DEP [7]. This effect is more pronounced when the solution is made using surfactants and has a high conductivity, whereas in low-conductivity solutions it is minimal due to the small change in the temperature profile because of the small amount of heat
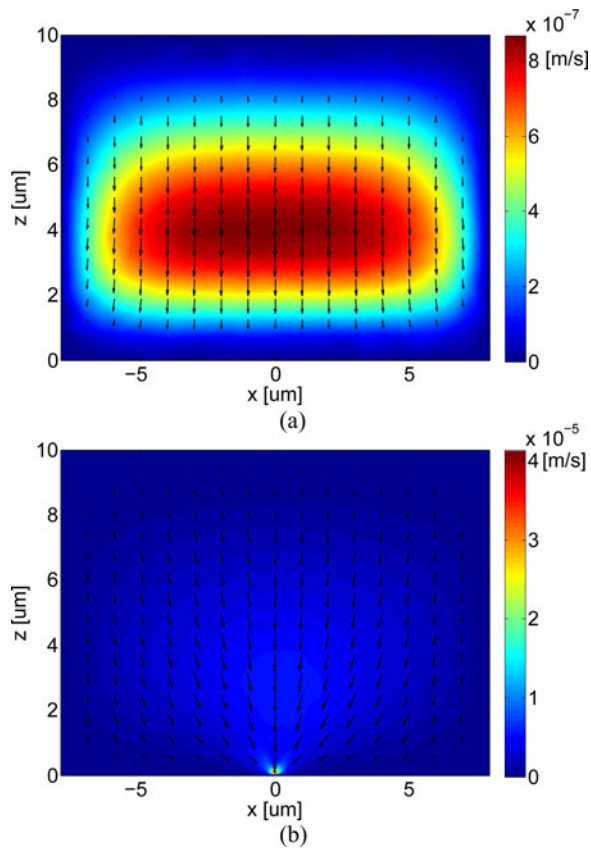
Fig. 8. Solution velocity due to the electrothermal force in a plane in the middle of the two electrodes: (a) no CNT deposited and (b) one CNT bridging.

generated by Joule heating in the solution. Although the solution used in the experiments reported here had low conductivity, the electrothermal force could be significant in the case of a nanotube bridging the two electrodes. The high current passing through the CNT, plus the defect prone structure of solution processed nanotubes, can potentially lead to the generation of nonnegligible amounts of heat and a high temperature gradient during the DEP experiment. To examine this possibility, an estimate of the temperature of the bridging CNT was needed.

The temperature of a CNT conducting current on a substrate was estimated by Pop *et al*. [18]. They showed that, for the largest part of the CNT structure on the surface, the temperature difference could be obtained from p/g, where p is the Joule heating rate per unit length and g is the net heat loss rate to the substrate per unit length. It was stated that g depends primarily on the interface and not on the thermal conductivity of the substrate. In order to obtain a rough estimate of the temperature of a nanotube conducting current in a solution, we assumed the heat loss rate to be double the case when the CNT is in air. The total resistance of a typical CNT device was measured to be around 5 MΩ. The average resistivity of a solution processed metallic CNT per μm of length is estimated to be 200 ± 10 kΩ [19]. p is equal to the square of current times the resistance per unit length. The current itself can be calculated by the division of the rms value of the voltage over the total resistance. The resulting temperature change was found to be around 0.18 K.

Fig. 8 demonstrates the temperature profile and the electrothermal motion in the solution with and without a nanotube bridging the two electrodes. Although the change in the temperature because of the presence of the conducting CNT considerably increases the electrothermal motion of the solution (the maximum increases from less than 1 to more than 40 μm/s on the plane of Fig. 8), this force is still negligible compared to the DEP force that the nanotubes experience (the maximum of DEP velocity is around 1.5 mm/s on the same plane), as seen by comparison with the velocity values shown in Figs. 3–6, which are primarily due to DEP. (It should be noted that all of the simulation results (Figs. 3–6) include both the DEP and the electrothermal induced movement of the nanotubes in the solution; however, as discussed, the main driving force is DEP).

IV. SUMMARY

In summary, CNTs form stripes during DEP deposition on wide electrodes due to changes in the electric field pattern because of the already deposited nanotubes. The process starts by the deposition of a few nanotubes on the edges of the electrodes. The DEP force is considerably enhanced around the tip of half bridging nanotubes and, therefore, other nanotubes are attracted and deposited in alignment and connection with them. The CNT bridges between the two electrodes push most of the suspended ones away laterally. On the other hand, a downward force pushes the suspended CNTs toward a bridging nanotube if they are close enough to it. The result of these interactions is the formation of stripes of nanotubes between the two electrodes. This effect is more pronounced for devices with larger gap distances.

The DEP force plays the dominant role in CNT pattern formation and the thermally-induced solution movement does not affect the final results for low conductivity solutions, even when a CNT conducts current and warms up as a result of Joule heating. In such a case, the electrothermal agitation increases considerably compared to the situation where there is no connection between the opposite electrodes, but still cannot take away from the dominance of the DEP.

REFERENCES

[1] R. Pething, "Review article- dielectrophoresis: Status of the theory, technology, and applications," *Biomicrofluidics*, vol. 4, pp. 022811-1–022811-35, 2010.

[2] C. Zhang, K. Khoshmanesh, A. Mitchell, and K. Kalantar-zadeh, "Dielectrophoresis for manipulation of micro/nano particles in microfluidic systems," *Anal. Bioanal. Chem.*, vol. 396, pp. 401–420, 2010.

[3] R. Martinez-Duarte, "Microfabrication technologies in dielectrophoresis applications: A review," *Electrophoresis*, vol. 33, pp. 3110–3132, 2012.

[4] H. Seo, C. Han, D. Choi, K. Kim, and Y. Lee, "Controlled assembly of single SWNTs bundle using dielectrophoresis," *Microelectron. Eng.*, vol. 81, pp. 83–89, 2005.

[5] R. Krupke, S. Linden, M. Rapp, and F. Hennrich, "Thin films of metallic carbon nanotubes prepared by dielectrophoresis," *Adv. Mater.*, vol. 18, pp. 1468–1470, 2006.

[6] S. Banerjee, B. E. White, L. Huang, B. J. Rego, S. O'Brien, and I. P. Herman, "Precise positioning of single-walled carbon nanotubes by AC dielectrophoresis," *J. Vac. Sci. Technol. B*, vol. 24, pp. 3173–3178, 2006.

[7] A. Kashefian Naieni and A. Nojeh, "Effect of solution conductivity and electrode shape on the deposition of carbon nanotubes from solution

using dielectrophoresis," *Nanotechnology*, vol. 23, pp. 495606-1–495606-9, 2012.

[8] S. Shekhar, P. Stokes, and S. Khondaker, "Ultrahigh density alignment of carbon nanotube arrays by dielectrophoresis," *ACS Nano*, vol. 5, pp. 1739–1746, 2011.

[9] P. Stokes, E. Silbar, Y. M. Zayas, and S. I. Khondaker, "Solution processed large area field effect transistors from dielectrophoreticly aligned arrays of carbon nanotubes," *Appl. Phys. Lett.*, vol. 94, pp. 113104-1–113104-3, 2009.

[10] A. H. Monica, S. J. Papadakis, R. Osiander, and M. Paranjape, "Wafer-level assembly of carbon nanotube networks using dielectrophoresis," *Nanotechnology*, vol. 19, pp. 085303-1–085303-5, 2008.

[11] A. Vijayaraghavan, S. Blatt, D. Wiessenberger, M. Oron-Carl, F. Hennrich, D. Gerthsen, H. Hahn, and R. Krupke, "Ultra-large-scale directed assembly of single-walled carbon nanotube devices," *Nano Lett.*, vol. 7, pp. 1556–1560, 2007.

[12] A. Kashefian Naieni and A. Nojeh, "Investigation of the dynamics of carbon nanotube deposition in dielectrophoresis," in *Proc. IEEE 5th Int. Nanoelectron. Conf.*, Singapore, 2013, pp. 52–55.

[13] (2013). [Online]. Available: http://www.nano-lab.com

[14] (2013). [Online]. Available: http://www.comsol.com

[15] B. R. Burg, V. Bianco, J. Schneider, and D. Poulikakos, "Electrokinetic framework of dielectrophorestic deposition devices," *J. Appl. Phys.*, vol. 107, pp. 124308-1–124308-11, 2010.

[16] Q. Cao, S. Han, G. S. Tulevski, A. D. Franklin, and W. Haensch, "Evaluation of field-effect mobility and contact resistance of transistors that use solution-processed single-walled carbon nanotubes," *ACS Nano*, vol. 6, pp. 6471–6477, 2012.

[17] Z. Chen, J. Appenzeller, J. Knoch, Y. Lin, and P. Avouris, "The role of metal−nanotube contact in the performance of carbon nanotube field-effect transistors," *Nano Lett.*, vol. 5, pp. 1497–1502, 2005.

[18] E. Pop, D. A. Mann, K. E. Goodson, and H. Dai, "Electrical and thermal transport in metallic single-wall carbon nanotubes on insulating substrates," *J. Appl. Phys.*, vol. 101, pp. 093710-1–093710-10, 2007.

[19] Q. Cao, S. Han, G. S. Tulevski, A. D. Franklin, and W. Haensch, "Evaluation of field-effect mobility and contact resistance of transistors that use solution-processed single-walled carbon nanotubes," *ACS Nano*, vol. 6, pp. 6471–6477, 2012.

Ali Kashefian Naieni (S'04) received the B.S. degree from Shiraz University, Shiraz, Iran, in 2005 and the M.S. degree from Sharif University of Technology, Tehran, Iran, in 2007 and is currently pursuing the Ph.D. degree at the University of British Columbia, Vancouver, BC, Canada.

His research interests include microfabrication technology; vacuum electronics; and modeling, simulation, fabrication and characterization of nano-material based electronic devices.

Alireza Nojeh (M'07) received the B.S. and M.S. degrees in electrical engineering from Sharif University of Technology, Tehran, Iran, in 1997 and 1999, respectively, the D.E.A. degree in electronics/optoelectronics from the University of Paris XI, Orsay, France, in 2000, and the Ph.D. degree in electrical engineering from Stanford University, Stanford, CA, USA, in 2006.

He is currently an Associate Professor of electrical and computer engineering at the University of British Columbia, Vancouver, BC, Canada. His research interests include nanotechnology, in particular carbon nanotube devices, electron sources, vacuum electronics, and electron microscopy, micro/nanofabrication, modeling, simulation of nanoscale structures, solid-state electronics, and opto-electronics.

Dr. Nojeh is also a Member of the American Vacuum Society.